

Study of the η -nucleus interaction in the $pd \rightarrow {}^3\text{He}\eta$ reaction near threshold

K. P. Khemchandani¹, N. G. Kelkar² and B. K. Jain³

Nuclear Physics Division, Bhabha Atomic Research Centre,
Mumbai 400085, India

Abstract

A detailed study of the effect of the η -nucleus final state interaction (FSI) in the $pd \rightarrow {}^3\text{He}\eta$ reaction close to threshold is presented. The FSI is incorporated through a T-matrix for η - ${}^3\text{He}$ elastic scattering, constructed using few body equations. This T-matrix accounts for off-shell and binding effects in η -nucleus scattering. The energy dependence of the data on the $pd \rightarrow {}^3\text{He}\eta$ reaction near threshold is reproduced only after including the FSI. The off-shell and binding effects in η - ${}^3\text{He}$ scattering are found to be important. Given the uncertainty in the knowledge of the elementary η -nucleon interaction, the sensitivity of the $pd \rightarrow {}^3\text{He}\eta$ cross section to different prescriptions of the elementary t-matrix, $t_{\eta N \rightarrow \eta N}$ is also discussed.

PACs numbers: 13.75.-n, 25.40.Ve, 25.10.+s

Keywords: final state interaction, η nucleus interaction, η meson production

1 Introduction

Experimental data on the $pd \rightarrow {}^3\text{He}\eta$ reaction close to threshold have revealed some surprising features [1, 2]. In spite of the large momentum transfer involved in η production as compared to that in pion production, the cross section for $pd \rightarrow {}^3\text{He}\eta$ is large and comparable with that for $pd \rightarrow {}^3\text{He}\pi^0$. The energy dependence of the two reactions near threshold is also very different. The $pd \rightarrow {}^3\text{He}\eta$ reaction shows a much rapid variation, with the

¹email: kanchanp@magnum.barc.ernet.in

²email: ngkelkar@apsara.barc.ernet.in

³email: brajesh_jain@vsnl.com

threshold amplitude falling by a factor of 3.75 over an η centre of mass momentum of 75 MeV/c.

The observed features of the $pd \rightarrow {}^3\text{He}\eta$ reaction have been attributed to the strong final state η -nucleus interaction. This reaction was studied in Ref. [3], where the final state interaction (FSI) was incorporated in an approximate way through an enhancement factor. The cross section was factorized in terms of the amplitude for the reaction $pd \rightarrow {}^3\text{He}\eta$ with plane waves for the η ${}^3\text{He}$ in the final state and an S-wave FSI factor written in terms of the on-shell η -nucleon amplitude. The energy dependence of the cross section data was reproduced, though its predicted absolute value was lower by a factor of 2.5. In yet another work [4], the scattering length of the η meson on helium was calculated using multiple scattering theory, which was then used to calculate the FSI factor for the $pd \rightarrow {}^3\text{He}\eta$ cross section. The FSI factor with an η -nucleon scattering length $a_{\eta N} = (0.291, 0.36)$ leading to $a_{\eta {}^3\text{He}} = (-0.89, 1.8)$ was found to give a good fit to the $pd \rightarrow {}^3\text{He}\eta$ data.

The $pd \rightarrow {}^3\text{He}\eta$ reaction at threshold and higher energies has also been studied theoretically to investigate the reaction mechanism involved [5, 6, 7]. Due to the large mass of the η meson, the momentum transfer involved in this reaction is large. It is 900 MeV/c at threshold and reduces to 500 MeV/c by about 1 GeV above threshold. As a result of this, it was shown in Ref. [5] that the three-body mechanism which allows the momentum transfer to be shared amongst three nucleons dominates. The one and two body mechanisms were found to underestimate the experimental cross sections by more than two orders of magnitude. The three nucleons share the large momentum transfer through a two step process where the incident proton interacts with a nucleon in the deuteron to produce a pion which then interacts with the other nucleon in the deuteron to produce an η meson. The $pd \rightarrow {}^3\text{He}\eta$ reaction, thus, proceeds via the $NN \rightarrow \pi d$ and $\pi N \rightarrow \eta N$ reactions. Though the $pd \rightarrow {}^3\text{He}\eta$ reaction can in principle proceed through the one and two body mechanism, considering the support in existing literature [5, 8] for the three body mechanism and the fact that the low momentum components of the nuclear wave function are picked up in this way, at least at energies very close to threshold it seems justified to consider this mechanism to be the only major reaction mechanism for the $pd \rightarrow {}^3\text{He}\eta$ reaction.

In the present work we study the $pd \rightarrow {}^3\text{He}\eta$ reaction near threshold using the three body mechanism mentioned above. Our main objective is to investigate the FSI in this reaction in a rigorous way. The above mentioned

theoretical works in the literature either neglect the FSI or incorporate it in an approximate way using on-shell amplitudes. We express the η ^3He relative wave function in terms of the Lippmann Schwinger equation involving the T-matrix for η ^3He elastic scattering. This T-matrix is evaluated using a method of few body equations [9, 10, 11] which will be described in detail in the next section.

In section 2 we present the formalism for the calculation of the $pd \rightarrow ^3\text{He}\eta$ cross section including the FSI. The production mechanism for $pd \rightarrow ^3\text{He}\eta$ reaction within a two-step model is described in section 3. In section 4 we present the results. We reproduce the shape and magnitude of the experimentally measured scattering amplitude. The off-shell effects in η ^3He scattering are found to be important in producing the energy dependence of the cross section.

2 Final state interaction

The transition matrix for the reaction $pd \rightarrow ^3\text{He}\eta$, which includes the interaction between the η meson and ^3He is given by,

$$T = \langle \Psi_{\eta^3\text{He}}^-(\vec{k}_\eta); m_3 | T_{pd \rightarrow ^3\text{He}\eta} | \vec{k}_p; m_1 m_2 \rangle \quad (1)$$

where m_1 , m_2 and m_3 are the spin projections of the proton, deuteron and helium respectively. \vec{k}_p and \vec{k}_η are the momenta of the particles in the initial and final states. The final state η ^3He wave function $\Psi_{\eta^3\text{He}}^{-*}$ consists of a plane wave and a scattered wave, and can be written as,

$$\langle \Psi_{\eta^3\text{He}}^- | = \langle \vec{k}_\eta | + \int \frac{d\vec{q}}{(2\pi)^3} \frac{\langle \vec{k}_\eta | T_{\eta^3\text{He}} | \vec{q} \rangle}{E(k_\eta) - E(q) + i\epsilon} \langle \vec{q} | \quad (2)$$

where $T_{\eta^3\text{He}}$ is the T-matrix for η ^3He elastic scattering. Replacing the above wave function in Eq. (1), we get,

$$T = \langle \vec{k}_\eta; m_3 | T_{pd \rightarrow ^3\text{He}\eta} | \vec{k}_p; m_1 m_2 \rangle + \sum_{m'_3} \int \frac{d\vec{q}}{(2\pi)^3} \frac{\langle \vec{k}_\eta; m_3 | T_{\eta^3\text{He}} | \vec{q}; m'_3 \rangle}{E(k_\eta) - E(q) + i\epsilon} \langle \vec{q}; m'_3 | T_{pd \rightarrow ^3\text{He}\eta} | \vec{k}_p; m_1 m_2 \rangle \quad (3)$$

The matrix elements $\langle |T_{pd \rightarrow {}^3\text{He}\eta} \rangle$ in the above equation correspond to the Born amplitude for the $pd \rightarrow {}^3\text{He}\eta$ reaction. We calculate these matrix elements using a two step model which will be discussed in the next section.

The T-matrix, $T_{\eta{}^3\text{He}}$, in Eq. (3) for η ${}^3\text{He}$ elastic scattering is evaluated using four particle equations for the $\eta(3N)$ system. For practical convenience, the evaluation of $T_{\eta{}^3\text{He}}$ is done within a Finite Rank Approximation (FRA) approach. This means that the nucleus in the elastic meson-nucleus scattering is always in its ground state. The shortcomings of the FRA for the η -deuteron system have been investigated in Ref. [12]. However, for the low energies concerned in this work and also as mentioned in Ref. [12], it seems justified to use the FRA for the $\eta - {}^3\text{He}$ system. We write the target Hamiltonian H_A as,

$$H_A \approx \varepsilon |\psi_0 \rangle \langle \psi_0| \quad (4)$$

where ψ_0 is the nuclear ground state wave function and ε the binding energy.

Within this approximation, the η ${}^3\text{He}$ T-matrix is given as [9, 10, 11],

$$\begin{aligned} T(\vec{k}', \vec{k}; z) &= \langle \vec{k}'; \psi_0 | T^0(z) | \vec{k}; \psi_0 \rangle + \\ &\varepsilon \int \frac{d\vec{k}''}{(2\pi)^3} \frac{\langle \vec{k}'; \psi_0 | T^0(z) | \vec{k}''; \psi_0 \rangle}{(z - \frac{k''^2}{2\mu})(z - \varepsilon - \frac{k''^2}{2\mu})} T(\vec{k}'', \vec{k}; z) \end{aligned} \quad (5)$$

where $z = E - |\varepsilon| + i0$. E is the energy associated with η -nucleus relative motion and μ is the reduced mass of the η -nucleus system. The operator T^0 describes the scattering of η meson from nucleons fixed in their space position within the nucleus. The matrix elements for T^0 are given as,

$$\langle \vec{k}'; \psi_0 | T^0(z) | \vec{k}; \psi_0 \rangle = \int d\vec{r} |\psi_0(\vec{r})|^2 T^0(\vec{k}', \vec{k}; \vec{r}; z) \quad (6)$$

where,

$$T^0(\vec{k}', \vec{k}; \vec{r}; z) = \sum_{i=1}^A T_i^0(\vec{k}', \vec{k}; \vec{r}_i; z) \quad (7)$$

T_i^0 is the t-matrix for the scattering of the η -meson from the i^{th} nucleon in the nucleus, with the rescattering from the other (A-1) nucleons included. It is given as,

$$T_i^0(\vec{k}', \vec{k}; \vec{r}_i; z) = t_i(\vec{k}', \vec{k}; \vec{r}_i; z) + \int \frac{d\vec{k}''}{(2\pi)^3} \frac{t_i(\vec{k}', \vec{k}''; \vec{r}_i; z)}{z - \frac{k''^2}{2\mu}} \sum_{j \neq i} T_j^0(\vec{k}'', \vec{k}; \vec{r}_j; z) \quad (8)$$

The t-matrix for elementary η -nucleon scattering, t_i , is written in terms of the two body ηN matrix $t_{\eta N}$ as,

$$t_i(\vec{k}', \vec{k}; \vec{r}_i; z) = t_{\eta N}(\vec{k}', \vec{k}; z) \exp[i(\vec{k} - \vec{k}') \cdot \vec{r}_i] \quad (9)$$

The ${}^3\text{He}$ wave function ψ_0 , required in the calculation of $T_{\eta{}^3\text{He}}$ is taken to be of the Gaussian form.

Since there exists a lot of uncertainty in the knowledge of the η -Nucleon interaction, we use three different prescriptions of the η -N t-matrix, $t_{\eta N \rightarrow \eta N}$, leading to different values of the η -N scattering length. We give a brief description of these models of $t_{\eta N \rightarrow \eta N}$ below. The elementary matrix, $t_{\eta N \rightarrow \eta N}$ is then used in the evaluation of the T-matrix for η ${}^3\text{He}$ scattering. In Ref. [13] a coupled channel t-matrix including the πN and ηN channels with the S_{11} - ηN interaction playing a dominant role was constructed. The t-matrix thus consisted of the meson - N^* vertices and the N^* propagator as given below:

$$t_{\eta N \rightarrow \eta N}(k', k; z) = \frac{g_{N^*} \beta^2}{(k'^2 + \beta^2)} \tau_{N^*}(z) \frac{g_{N^*} \beta^2}{(k^2 + \beta^2)} \quad (10)$$

with,

$$\tau_{N^*}(z) = (z - M_0 - \Sigma_\pi(z) - \Sigma_\eta(z) + i\epsilon)^{-1} \quad (11)$$

where $\Sigma_\alpha(z)$ ($\alpha = \pi, \eta$) are the self energy contributions from πN and ηN loops. The parameters of this model were chosen to produce an ηN scattering length, $a_{\eta N} = (0.75, 0.27)$ fm which is in agreement with some other analyses available in literature [14, 15]. We will refer to this parameter set as ‘Fix *et al.* (I)’ while discussing the results.

In Ref. [13] the authors also perform calculations with the choice of meson-nucleon cut-off parameters as in Ref. [16]. These parameters lead to $a_{\eta N} = (0.88, 0.41)$ fm. We refer to this parameter set as ‘Fix *et al.* (II)’. We present our calculations for the $pd \rightarrow {}^3\text{He} \eta$ reaction with the t-matrix of Ref. [13] using the two different sets of parameters mentioned above.

We also present results using the η -N t-matrix of Ref. [17] which gives a much smaller value of $a_{\eta N}$, namely, $a_{\eta N} = (0.28, 0.19)$ fm. In this model the πN , ηN and $\pi \Delta$ channels were treated in a coupled channels formalism. It is important to note that the parameters in all the coupled channel t-matrices mentioned above are adjusted to reproduce the data on the $\pi N \rightarrow \eta N$ reaction, but the values of $a_{\eta N}$ deduced from them are different.

3 Production mechanism

As mentioned in the Introduction, we assume the η production in $pd \rightarrow {}^3\text{He}\eta$ to proceed through a two-step process via the $NN \rightarrow \pi d$ and $\pi N \rightarrow \eta N$ reactions as shown in Fig. 1. The amplitude for the $pd \rightarrow {}^3\text{He}\eta$ reaction appearing in Eq. (3) can be written within this model as,

$$\begin{aligned} \langle |T_{pd \rightarrow {}^3\text{He}\eta}| \rangle = & i \int \frac{d\vec{p}_1}{(2\pi)^3} \frac{d\vec{p}_2}{(2\pi)^3} \sum_{int m's} \langle pn | d \rangle \langle \pi^+ d | T_{pp \rightarrow \pi^+ d} | pp \rangle \quad (12) \\ & \times \frac{1}{(k_\pi^2 - m_\pi^2 + i\epsilon)} \langle \eta p | T_{\pi N \rightarrow \eta p} | \pi^+ n \rangle \langle {}^3\text{He} | pd \rangle \end{aligned}$$

where the sum runs over the spin projections of the intermediate particles.

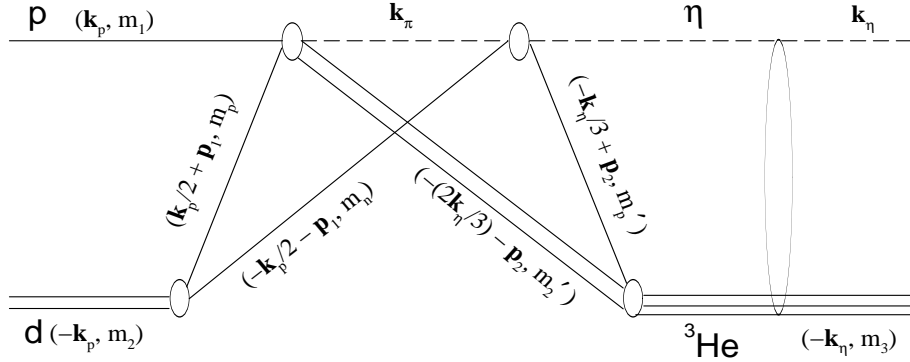


Figure 1: Diagram of η production in the $pd \rightarrow {}^3\text{He}\eta$ reaction with a two-step process. The ellipse indicates the final state interaction of ${}^3\text{He}$ and η .

The spin projections and momenta of the interacting particles are as shown in Fig. 1. k_π is the four momentum of the intermediate pion which could either be π^+ or π^0 . In the case of an intermediate π^0 , the matrix element for $pd \rightarrow {}^3\text{He}\eta$ is half of that written above for π^+ . Hence we calculate the T-matrix as in Eq. (12) and multiply it by a factor of 3/2 to account for the intermediate π^0 . Each of the individual matrix elements in the above equation is expressed in terms of partial wave expansions. The matrix elements for the $pp \rightarrow \pi^+ d$ reaction, parametrized in terms of the available experimental data are taken from Ref. [18]. For the $\pi^+ n \rightarrow \eta p$ reaction, we use the coupled channel t-matrix of Ref. [17], mentioned in the previous section. The matrix elements

$\langle pn|d \rangle$ and $\langle {}^3\text{He}|pd \rangle$ consist of the deuteron and helium wave functions in momentum space. We use the deuteron wave function from Ref. [19] where an analytical parametrization of it was done with a Paris potential. This wave function reproduces the known low energy properties and the electromagnetic form factor of the deuteron well. For the ${}^3\text{He}$ wave function, we use the parametrization given in Ref. [20]. The values of the parameters in [20] were obtained by fitting the wave function to the variational calculations of Schiavilla *et al.* [21] using the Urbana force. The details of Eq. (12) are given in the appendix.

4 Results and Discussion

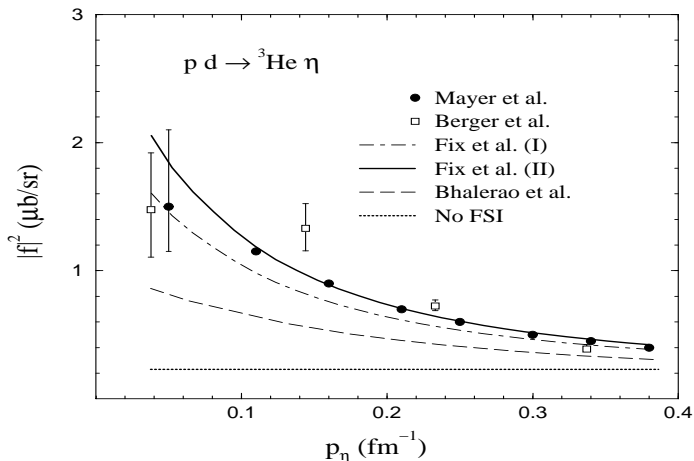


Figure 2: The square of the $pd \rightarrow {}^3\text{He}\eta$ amplitude defined in Eq. (13) as a function of the η momentum in the centre of mass. The data is from Refs [1, 2]. The dotted line is the calculation of the present work without including the FSI. The solid, dash-dotted and dashed lines are the calculations including FSI with different prescriptions of elementary t-matrices.

The reaction $pd \rightarrow {}^3\text{He}\eta$ has been studied at Saturne [1, 2] for proton energies between 0.2 and 11 MeV above threshold. Taking out the phase

space factor, the spin averaged amplitude can be defined as,

$$|f|^2 = \frac{k_p}{k_\eta} \cdot \frac{d\sigma}{d\Omega_{cm}} \quad (13)$$

where k_p and k_η are the proton and η momenta in the centre of mass system. The data on $|f|^2$ (see Fig. 2) drops rapidly (by about a factor of 3.75) from threshold to 0.4 fm^{-1} momentum (corresponding to 11 MeV energy) above threshold. In Fig. 2 we compare our calculations of $|f|^2$ (at $\theta_\eta = 180^\circ$) with and without the inclusion of the η ^3He final state interaction (FSI), with the data from Refs [1, 2]. The dotted line in Fig. 2 is our calculation without FSI and can be seen to be a constant as a function of energy. The dash-dotted, solid and dashed curves are the results obtained using the t-matrix of Ref. [13], with parameter sets (I) and (II), and that of Ref. [17] respectively. We see that the FSI is responsible for changing the shape of $|f|^2$ from a constant to a rapidly falling one as a function of energy.

In what follows, we shall study the off shell and the binding energy effects in the FSI. We also calculate the angular distribution and total cross-sections for the $pd \rightarrow ^3\text{He}\eta$ reaction. In all these calculations we use the prescription of Ref. [13] with parameter set (II) for the elementary t-matrix, $t_{\eta N \rightarrow \eta N}$. We arrive at the same results qualitatively, in all the calculations if we choose the parameter set (I) of the same t-matrix or the elementary matrix, $t_{\eta N \rightarrow \eta N}$ of Ref. [17].

In Fig. 3 we study the off-shell effects in the FSI. As seen in section 2, we describe the η ^3He final state interaction through an off-shell T-matrix for η ^3He scattering. Previous estimates of FSI in literature have been made using on-shell amplitudes and hence it is important to check the validity of such an approximation. The η ^3He T-matrix appears in an integral in Eq. (3) which can be split into the principal value and pole term. Retaining only the pole term in Eq. (3) and setting the principal value (which involves the off-shell η ^3He scattering) to zero, we get the dash dotted line in Fig. 3. The pole term alone is unable to reproduce the shape of the data and in fact reduces the magnitude of the results obtained without FSI. We find that $t_{\eta N \rightarrow \eta N}$ of Ref. [13], with parameter set (I) and (II) and that of Ref. [17] have similar on-shell behaviour meaning that the same dash dotted curve of Fig. 3 represents the pole term calculation for the 3 different prescriptions of $t_{\eta N \rightarrow \eta N}$. The solid line represents the full calculation using the prescription of Ref. [13] with parameter set (II) for the elementary t-matrix. Thus we see

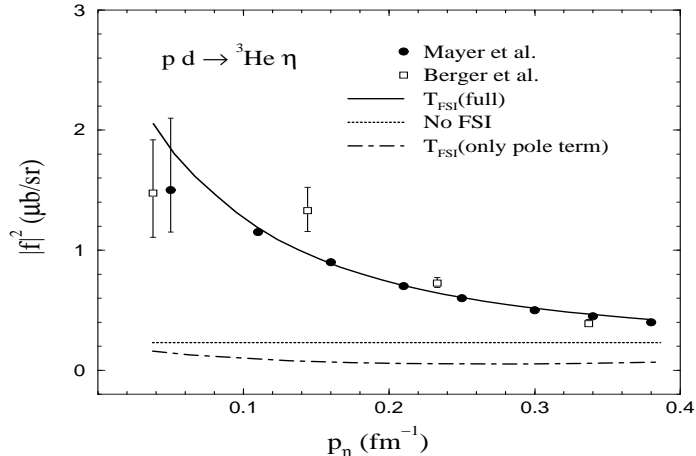


Figure 3: The solid and dotted line and the data are as in Fig. 2. The dash dotted line is the FSI calculation retaining only the pole term in Eq. (3). We have used the elementary t-matrix of Ref. [13] with parameter set (II).

that including the off shell effects produces the proper energy dependence of $|f|^2$ in addition to increasing its magnitude as compared to the pole term calculation. The other two prescriptions of $t_{\eta N \rightarrow \eta N}$ (Fix *et al.* (I) and Bhalerao *et al.*) show similar off-shell effects. However, as can be seen from the curves in Fig. 2, the increase in magnitude as compared to the pole term is smaller.

Next, in Fig. 4, we study the effect of the FSI on the angular distributions at different energies. As observed in Fig. 2 too, we see that the FSI increases the magnitude of the cross sections with the increase being maximum at threshold (Fig. 4a). The angular dependence of the cross sections without FSI (dashed lines) is isotropic at threshold and deviates by a small amount from the isotropy with increase in beam energy. The small anisotropy at a few MeV above threshold is somewhat amplified by the final state interaction. Thus, as one goes to higher energies (Fig. 4c), though the FSI does not increase the magnitude of the cross section too much, it does change the angular dependence.

In Fig. 5 we show the angle integrated total cross section as a function of beam energy. The total cross sections without FSI are shown by the dashed

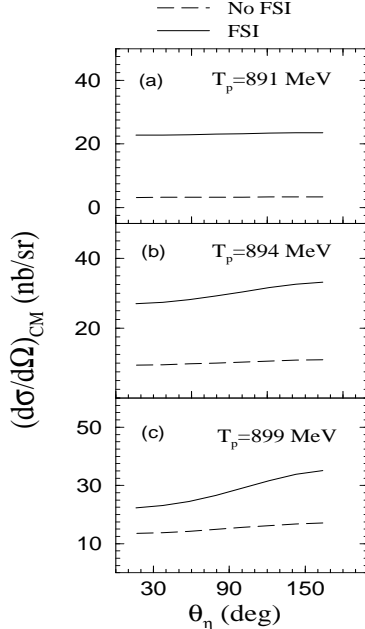


Figure 4: Angular distribution of η in the $pd \rightarrow {}^3\text{He}\eta$ reaction at different beam energies. The solid (dashed) curves are the calculations with (without) FSI included.

line. The solid line is obtained by numerically integrating the angular distribution with FSI included. The dash dotted curve indicates the total cross section calculated with FSI included but assuming the angular distribution to be isotropic (i.e. $\sigma_{tot} = 4\pi(d\sigma/d\Omega)_{\theta_\eta=180^\circ}$). The data of Ref. [1] seems to indicate a negligible forward-backward asymmetry (which is consistent with zero within 5% at all energies from 0 to 11 MeV above threshold) in the $pd \rightarrow {}^3\text{He}\eta$ reaction. Within the two-step FSI model of the present work, however, we find small deviations from isotropy at energies away from threshold. Since the total cross section assuming isotropic angular distribution gives better agreement with data, it seems that the two step model of the present work underestimates the cross section at forward angles. The data on the squared amplitude $|f|^2$ at 180° is however very well produced as seen earlier in Fig. 2.

Finally, in Fig. 6 we study the effects on the $pd \rightarrow {}^3\text{He}\eta$ reaction, of

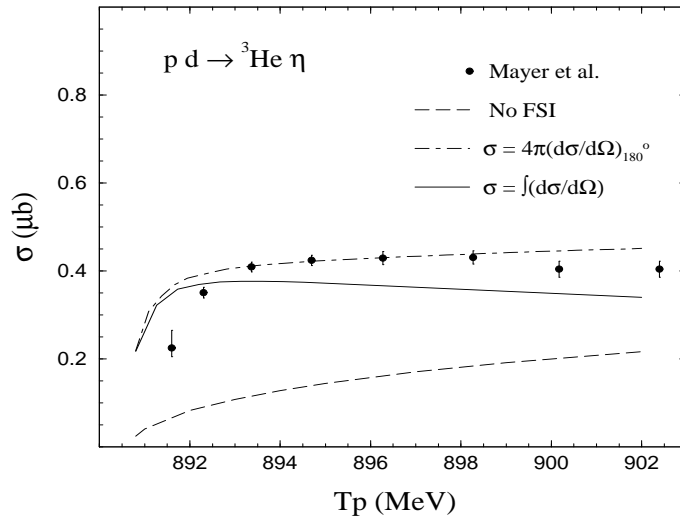


Figure 5: Total cross section for $p d \rightarrow {}^3\text{He } \eta$ as a function of beam energy. Solid curve is obtained by numerically integrating the calculated $d\sigma/d\Omega$ with FSI over all angles. The dash dotted curve is obtained by multiplying $d\sigma/d\Omega$ (with FSI) at 180° with 4π , thus assuming the angular distribution to be isotropic. The dashed curve is the calculation without FSI. The data is from Ref. [1].

including the FSI which incorporates the binding effects in ${}^3\text{He}$. Once again we plot the amplitude squared $|f|^2$ calculated for three different elementary t-matrices, $t_{\eta N \rightarrow \eta N}$. The solid curves are the calculations using $\varepsilon = -7.718$ MeV in Eq. (5) for $T_{\eta {}^3\text{He}}$. The dashed curves represent the calculation with $\varepsilon = 0$, i.e. no binding effects in the final state interaction. The calculated results without the binding effects are larger than those which include them. The magnitude of the increase, however, depends upon the elementary t-matrix, $t_{\eta N \rightarrow \eta N}$, under consideration. It is nearly a factor of 2 when we use the t-matrix of Ref. [13], with parameter set (I), a factor of 1.25 when we use the same t-matrix with parameter set (II) and negligibly small for the t-matrix of Ref. [17].

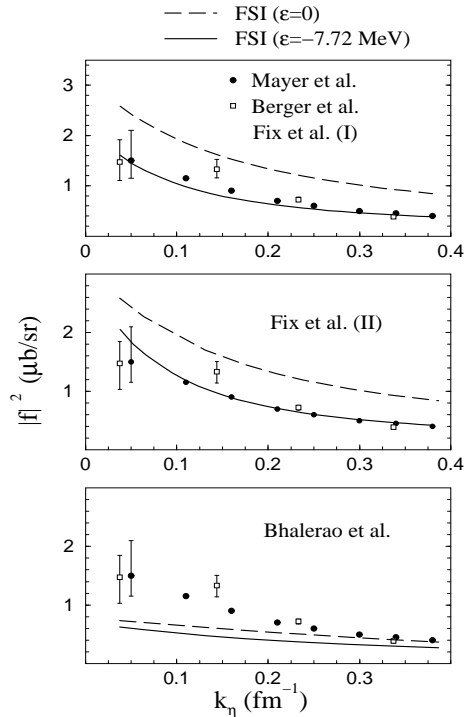


Figure 6: Effects of including the binding energy of ${}^3\text{He}$ in the calculation of FSI between ${}^3\text{He}$ and η . The solid and dashed curves are calculations including FSI with the binding energy $\varepsilon = -7.718$ and zero respectively (see Eq.(5)). The effect is shown for three different elementary t-matrices, $t_{\eta N \rightarrow \eta N}$.

5 Summary

The $pd \rightarrow {}^3\text{He}\eta$ reaction has been studied in the present work within a two step model, incorporating the final state interaction (FSI) of the ${}^3\text{He}$ nucleus and η meson in a rigorous way. The peculiar behaviour of the cross section for this η producing reaction as compared to a similar pion production reaction $pd \rightarrow {}^3\text{He}\pi^0$ is seen to originate due to the interaction between ${}^3\text{He}$ and η . The FSI changes the energy dependence of the squared amplitude from a constant (without FSI) to one which falls by a factor of about 4, from threshold to 11 MeV above threshold. We incorporate the FSI through an off-shell T-matrix for η - ${}^3\text{He}$ elastic scattering. This T-matrix is evaluated by numerically solving few body equations which include the nuclear binding

effects. Both the off-shell as well binding effects in η ^3He scattering are found to be important in the calculation of the $pd \rightarrow ^3\text{He}\eta$ reaction near threshold. Earlier investigations of this reaction involving on-shell and approximate ways of calculating the FSI should hence be treated with caution.

The η nucleus interaction has generated a lot of interest in the past few years, particularly due to the possibility of forming η mesic nuclei. Since it is difficult to obtain data on elementary η nucleon scattering, little is known about the ηN interaction. The scattering length in ηN scattering is a much debated quantity and different estimates and limiting values (for the possible formation of an η mesic nucleus) of this parameter exist in literature. Within the models used in the present work we find that values of the ηN scattering length, $\text{Re } a_{\eta N} \sim 0.75$ to 0.9 and $\text{Im } a_{\eta N} \sim 0.3$ to 0.4 lead to a good reproduction of the $pd \rightarrow ^3\text{He}\eta$ data near threshold.

Acknowledgements

The authors wish to thank Prof. R. A. Arndt for providing the code required for the calculation of the $pp \rightarrow \pi^+ d$ amplitudes and Profs. R. S. Bhalerao and E. Oset for useful discussions. One of the authors (K.P.K.) gratefully acknowledges the award of a research fellowship from the Department of Atomic Energy of the Government of India.

Appendix

In what follows, we discuss in detail the constituents of the Born amplitude (Eq. (12)) for the $pd \rightarrow ^3\text{He}\eta$ reaction. To start with, we write the deuteron wave function in Eq. (12) as,

$$\begin{aligned} \sum \langle pn | d \rangle = & \frac{1}{\sqrt{2}} \left\{ \sum_{m_n} \langle 1/2 m_p 1/2 m_n | 1 m_2 \rangle \frac{\phi_0^d(p_1)}{\sqrt{4\pi}} \right. \\ & \left. + \sum_{m_l} \langle 1/2 m_p 1/2 m_n | 1 M_s \rangle \langle 1 M_s 2 m_l | 1 m_2 \rangle Y_{2,m_l}(\hat{p}_1) \phi_2^d(p_1) \right\} \end{aligned} \quad (\text{A.1})$$

where m_n and m_p are the spin projections of the off-shell neutron and proton respectively in the intermediate state and m_2 is the spin projection of the target deuteron. The factor $\frac{1}{\sqrt{2}}$ comes from isospin overlap. $\phi_l^d(p_1)$ is the

deuteron wave function in the l^{th} partial wave and \vec{p}_1 is the relative momentum of the p-n pair inside the deuteron. Writing

$$\phi_0^d(p_1) = (2/\pi)^{\frac{1}{2}} \sum_{j=1}^n \frac{C_j}{p_1^2 + m_j^2} \quad (\text{A.2})$$

$$\phi_2^d(p_1) = (2/\pi)^{\frac{1}{2}} \sum_{j=1}^n \frac{D_j}{p_1^2 + m_j^2}, \quad (\text{A.3})$$

the parameters C_j , D_j and m_j for the Paris potential are given in Ref. [19]. The ${}^3\text{He}$ wave function is written as,

$$\begin{aligned} \sum_{m'_2, m'_p} \langle {}^3\text{He} | p d \rangle = \sum_{m'_2, m'_p} \langle 1 m'_2 \ 1/2 m'_p | 1/2 m_3 \rangle \frac{\chi_0(p_2)}{\sqrt{4\pi}} + \quad (\text{A.4}) \\ \sum_{m'_i} \langle 1 m'_2 \ 1/2 m'_p | 3/2 m \rangle \langle 2 m'_i \ 3/2 m | 1/2 m_3 \rangle \chi_2(p_2) Y_{2, m'_i}(\hat{p}_2) \end{aligned}$$

where m'_2 and m'_p are the spin projections of the off-shell deuteron and proton respectively. The spin projection of ${}^3\text{He}$ is m_3 as shown in Fig. 1. $\chi_l(p_2)$ is the helium wave function in the l^{th} partial wave and \vec{p}_2 is the relative momentum of the p-d pair inside ${}^3\text{He}$.

$$\chi_l(p_2) = \sum_{i=1}^n \frac{a_i}{p_2^2 + m_i^2} \quad (\text{A.5})$$

The parameters a_i and m_i given in Ref. [20] are chosen corresponding to p-d clustering in ${}^3\text{He}$. The normalization of the wave function is such that,

$$\int p_2^2 dp_2 \{ \chi_0(p_2)^2 + \chi_2(p_2)^2 \} = 1.5 \quad (\text{A.6})$$

The four momentum $k_\pi = \{ E_\pi, \vec{k}_\pi \}$ appearing in the pion propagator in Eq. (12) is written using energy and momentum conservation at the $\pi^+ n \rightarrow \eta p$ and $pp \rightarrow \pi^+ d$ vertices respectively. Thus,

$$E_\pi = E_\eta + \frac{1}{3}E_{He} - \frac{1}{2}E_d \quad (\text{A.7})$$

and

$$\vec{k}_\pi = \frac{\vec{k}_p}{2} + \frac{2}{3}\vec{k}_\eta + \vec{p}_1 + \vec{p}_2 \quad (\text{A.8})$$

References

- [1] B. Mayer et al., Phys. Rev. C 53 (1996) 2068.
- [2] J. Berger et al., Phys. Rev. Lett. 61 (1988) 919.
- [3] G. Fäldt and C. Wilkin, Nucl. Phys. A 587 (1995) 769.
- [4] S. Wycech, A. M. Green and J. A. Niskanen, Phys. Rev. C 52 (1995) 544.
- [5] J. M. Laget and J. F. Lecomte, Phys. Rev. Lett. 61 (1988) 2069.
- [6] L. A. Kondratyuk, A. V. Lado and Yu. N. Uzikov, Phys. Atom. Nucl 58 (1995) 473; Yad. Fiz. 58 (1995) 524; L. A. Kondratyuk and Yu. N. Uzikov, Phys. Atom. Nucl. 60 (1997) 468; Yad. Fiz. 60 (1997) 542; nucl-th/9510010.
- [7] A. B. Santra and B. K. Jain, Phys. Rev. C 64 (2001) 025201.
- [8] K. Kilian and H. Nann, in *Meson Production near Threshold*, ed. H. Nann and E. J. Stephenson, AIP Conf. Proc. 221 (1990) 185.
- [9] V. B. Belyaev, *Lectures on the theory of FEW BODY SYSTEMS*, Springer series in Nuclear and Particle Physics, 1990.
- [10] S. A. Rakityansky and S. A. Sofianos, Proceedings of The European Conference on Advances in nuclear physics and related areas, Thessaloniki-Greece, (1997) 570, Giahoudi-Giapouli Publishing, Thessaloniki, 1999.
- [11] S. A. Rakityansky, S. A. Sofianos, M. Braun, V. B. Belyaev and W. Sandhas, Phys. Rev. C 53 (1996) R2043;
S. A. Rakityansky, S. A. Sofianos, V. B. Belyaev and W. Sandhas, Few-Body Systems Suppl., 9 (1995) 227.
- [12] N. V. Shevchenko, S. A. Rakityansky, S. A. Sofianos, V. B. Belyaev and W. Sandhas, Phys. Rev. C 58 (1998) R3055.
- [13] A. Fix and H. Arenhövel, Nucl. Phys A 697 (2002) 277.
- [14] A. M. Green and S. Wycech, Phys. Rev. C 55 (1997) 2167.

- [15] Batinić, I. Dadić, I. Šlaus, A. Švarc, B. M. K. Nefkens and T. S. H. Lee, *Physica Scripta* 58 (1998) 15; nucl-th/9703023 (1997).
- [16] H. Garcilazo and M. T. Peña, *Phys. Rev. C* 63 (2001) 021001.
- [17] R. S. Bhalerao and L. C. Liu, *Phys. Rev. Lett.* 54 (1985) 865.
- [18] R. A. Arndt, I. Strakovsky, R. L. Workman and D. A. Bugg, *Phys. Rev. C* 48 (1993) 1926. The amplitudes can be obtained from the SAID program available on internet (<http://gwdac.phys.gwu.edu>). To access via telnet, connect to 'gwdac.phys.gwu.edu' with login 'said' and no password.
- [19] M. Lacombe, B. Loiseau, R. Vinh Mau, J. Côté, P. Pirés and R. de Tournell, *Phys. Lett. B* 101 (1981) 139.
- [20] J. F. Germond and C. Wilkin, *J. Phys. G* 14 (1988) 181.
- [21] R. Schiavilla, V. R. Pandharipande, R. B. Wiringa, *Nucl. Phys. A* 449 (1986) 219.